X-Ray Diffraction Topography

Pergamon
International
Library

B.K.TANNER *Lecturer in Physics, Durham University*

International
Series in the
Science of the
Solid State
Volume 10

X-RAY DIFFRACTION TOPOGRAPHY

by

B. K. TANNER, M.A., D. Phil.
Lecturer in Physics, Durham University

PERGAMON PRESS
OXFORD · NEW YORK · TORONTO · SYDNEY · PARIS · FRANKFURT

U. K.	Pergamon Press Ltd., Headington Hill Hall, Oxford OX3 0BW, England
U. S. A.	Pergamon Press Inc., Maxwell House, Fairview Park, Elmsford, New York 10523, U.S.A.
CANADA	Pergamon of Canada Ltd., P.O. Box 9600, Don Mills M3C 2T9, Ontario, Canada
AUSTRALIA	Pergamon Press (Aust.) Pty. Ltd., 19a Boundary Street, Rushcutters Bay, N.S.W. 2011, Australia
FRANCE	Pergamon Press SARL, 24 rue des Ecoles, 75240 Paris, Cedex 05, France
WEST GERMANY	Pergamon Press GmbH, 6242 Kronberg-Taunus, Pferdstrasse 1, Frankfurt-am-Main, West Germany

First edition 1976

Library of Congress Cataloging in Publication Data

Tanner, Brian Keith.
X-ray diffraction topography.

(I S science of the solid state; v. 10)
Includes bibliographical references.
1. X-ray crystallography. I. Title.
QD945.T36 1976 548'.83 75-45196
ISBN 0 08 019692 6

Printed in Great Britain by A. Wheaton & Co., Exeter

SERIES EDITOR'S PREFACE

X-ray topography is the latest in a long line of tools for the study of crystals which use X-ray diffraction. This is the first book devoted entirely to developing the theme of the principles and application of this technique and will fill a very real gap in the literature. It is assured of a ready welcome. I am particularly glad to welcome it into this series as it compliments existing and forthcoming volumes, particularly Crystal Growth, Oxide Semiconductors, and Defects and Surfaces in Semiconducting Materials and Devices.

Many laboratories interested in the study of solid state devices and the materials which go into them now have X-ray topographic facilities. The technique has proved useful in the study of dislocations and faults in metal crystals, semiconducting materials and bubble memory garnets as well as a wide range of other materials from natural diamonds to silicon integrated circuits. The quality of heterojunction lasers was improved when the behaviour of dislocations in the (Ga,Al)As layers was illuminated by X-ray topographic studies. It is a very powerful new tool for solid state scientists and crystal growers and is already well established for the assessment of crystal quality in a wide range of single crystal materials.

Dr. Brian Tanner is an acknowledged leader in the field although still quite a young man. He studied at Oxford before going to Durham to set up a laboratory for X-ray topography in the Department of Physics. He has given invited papers at several International Conferences and published over twenty research papers.

Brian Pamplin
January, 1976.
Scientific Advisers and Co.,
15 Park Lane,
Bath.

PREFACE

Although by no means a new technique, the use of X-ray topography is at present increasing rapidly, particularly as an aid to crystal growth studies and quality control of monolithic crystal devices. The technique is complementary to its cousin, transmission electron microscopy in that X-ray topography enables a thick, nearly perfect single crystal to be examined with a relatively poor resolution over a large area whereas electron microscopy necessarily uses thin specimens of quite high dislocation density and examines a very small area with excellent resolution.

Improvements in crystal growth techniques in the last five years have provided many new materials suitable for X-ray topographic study and in turn, X-ray topography has provided the crystal grower with valuable data on the quality of his products. The feed-back between topographer and crystal grower or device manufacturer has proved so successful that today X-ray topographic analysis is performed as a standard routine by many crystal growing groups and firms manufacturing integrated circuits. The production of highly perfect single crystals has permitted the observation of many new X-ray optical phenomena and the detailed experimental verification of the various theories of dynamical X-ray diffraction. Correspondingly, the newly discovered effects have been utilized to the benefit of the crystal grower and device manufacturer in the development of new techniques with greater sensitivity to lattice parameter changes. As much of modern electronic engineering relies heavily on highly perfect single crystals, X-ray topography has claim to an important place in the hierarchy of assessment techniques.

Yet, despite the complex interaction between X-ray topographer and crystal grower, there seems to exist a certain lack of awareness of the recent developments, the potential and the problems of X-ray topography amongst non-specialists. There is a feeling that X-ray topography is a black art, understood only by a few initiates. While several excellent review articles have appeared, their existence is not widely known and in the sixteen years since X-ray topography was developed in its modern high resolution form, no book has been published on the subject.

From discussions with my colleagues, I am convinced that there exists a need for an elementary treatment of X-ray topography, comprehensible to the non-specialist who may have much to gain from occasional use of the techniques and it is this gap that the present volume is intended to fill. The book falls roughly into three sections. It is not comprehensive and my apologies are extended to any of my colleagues who may feel that their work has been unjustly neglected. In the first section the basic theory necessary for the understanding of topographic contrast is presented together with the chief experimental techniques and an analysis of the types of contrast observed. The second section presents some applications of topography. Those considered are included as being typical or classic studies and illustrate the kind of information obtained from topography. The final section reviews the work on assessment of crystal perfection in direct relation to the growth process. This is an area where future development will be rapid

and it is hoped that the growth points are anticipated. Following each chapter, a selected bibliography of additional papers is included as an appendix. These are grouped according to the main subject headings treated in the text.

My thanks are extended to those of my colleagues throughout the world who have provided the photographs without which the text would be lifeless. In particular I would like to thank Dr. A.D. Milne for his thorough and constructively critical reading of the manuscript and Mrs. S.M. Naylor for typing the final copy of the text. I acknowledge with gratitude the support of my wife and family, to whom the book is dedicated.

LIST OF SYMBOLS COMMONLY USED IN THE TEXT

A	Angular amplification
$\underline{b}$	Burgers vector
$\overline{\beta}$	Ray path parameter
c	Velocity of light
C	Polarization factor
c_{ij}	Elastic constants
γ_o, γ_g	Cosines of angle between Bragg planes and beam directions
$\underline{D}$	Electric displacement
$\underline{D}_o$, $\underline{D}_g$	Component amplitudes of wavefields
d	Lattice plane spacing
δ, ε	Resolution
$\underline{E}$	Electric field
$\overline{\eta}$	Deviation parameter
F_g	Structure factor
$\underline{g}$, $\underline{h}$	Reciprocal lattice vectors
$\underline{H}$	Magnetic field
$\underline{k}$	Wavevector *in vacuo*
$\underline{K}_o$, $\underline{K}_g$	Wavevector in the crystal
λ	Wavelength
Λ_o	Dispersion surface diameter
μ	Absorption coefficient
$\underline{P}$	Poynting vector
$\overline{p}$	Energy flow parameter
R	Amplitude ratio of diffracted and transmitted waves
r_e	Classical electron radius
$\hat{s}_o, \hat{s}_g$	Unit vectors in the transmitted and diffracted beam directions
χ_o	Susceptibility
χ_g	Fourier component of susceptibility
θ_B	Bragg angle
$\Delta\theta$	Angular deviation from exact Bragg angle
$\underline{u}$	Atomic displacement, dislocation line direction
$\overline{V}_c$	Volume of unit cell
ω	Angular frequency
ξ_g	Extinction distance

ACKNOWLEDGMENTS

The following photographs are copyright material and are reproduced here by kind permission of the publishers and authors.

Cover and Fig. 6.2	*J. Crystal Growth* (1974) 24/25, 108.
Fig. 2.9(b,c)	*J. Crystal Growth* (1974) 24/25, 64.
Fig. 2.16	*Nature* (1968) 220, 652.
Fig. 3.3(a) and Fig. 7.2	*J. Appl. Phys.* (1973) 44, 3905.
Fig. 3.12	*J. Appl. Cryst.* (1974) 7, 372.
Fig. 4.1	*J. Mater. Sci.* (1972) 7, 531.
Fig. 4.2	*Phil. Mag.* (1975) 32, 283.
Fig. 4.4	*J. Appl. Cryst.* (1973) 6, 31.
Fig. 4.9	*J. Appl. Phys.* (1967) 38, 3495.
Fig. 4.10	*J. Crystal Growth* (1974) 24/25, 637.
Fig. 4.11	*Phil. Mag.* (1973) 28, 1015.
Fig. 5.3	*J. Crystal Growth* (1973) 18, 135.
Fig. 5.4	*Acta Cryst.* (1973) A29, 495.
Fig. 5.5	*J. Crystal Growth* (1974) 24/25, 541.
Fig. 5.7	*J. Crystal Growth* (1975) 29, 281.
Fig. 5.8	*J. Crystal Growth* (1975) 28, 77.
Fig. 6.1	*Appl. Phys. Lett.* (1969), 15, 258.
Fig. 7.4(a)	*J. Crystal Growth* (1974), 24/25, 527.

CONTENTS

CHAPTER 1

BASIC DYNAMICAL X-RAY DIFFRACTION THEORY

It is important from the outset to emphasize that X-ray topography is not concerned primarily with the study of surfaces. The full title, X-ray Diffraction Topography, is much clearer as it indicates that the topography we are studying is that of the diffracting planes in the crystal, not the topography of the exterior features. Of course, the contours of the crystal surfaces are important in determining the contrast on X-ray topographs, but this is of somewhat secondary importance to the contours of the crystal lattice planes. When we use the technique to observe dislocations, we are studying the topography of the lattice planes around the defect. We do this by recording the intensity of the X-rays diffracted from the deformed planes which differs from the intensity diffracted by the perfect crystal forming a localized image of the defect. Essentially, we are using the phenomenon of diffraction to probe the internal structure of the crystal. It is not, however, a point probe, and the interpretation of the observed contrast is far from trivial.

At the simplest level, we can obtain some insight into how dislocations are imaged in the following way. Consider a perfect crystal set to diffract monochromatic X-radiation of wavelength λ from a set of lattice planes spaced d. For a strong diffracted beam to emerge at angle $2\theta_B$ to the incident beam the well known Bragg relation applies. That is,

$$\lambda = 2d \sin \theta_B \tag{1.1}$$

It is clear that when the lattice spacing or lattice plane orientation varies locally, e.g. around a dislocation, the relation will not apply simultaneously to the perfect and distorted regions. Consequently there is a difference in intensity corresponding to the two regions, i.e. an image of the defect.

In order to interpret these changes in intensity, and more importantly, relate them to the lattice plane topography in a particular crystal under investigation, we need to know something about the theory of X-ray diffraction in solids. Now although an elementary treatment of X-ray diffraction may be found in many textbooks on solid state physics, the treatment is based on the KINEMATICAL approximation. In this situation, it is assumed that the amplitudes of the scattered waves are at all times small compared with the incident wave amplitude. For small crystals, of dimensions less than about a micrometre in diameter, and in heavily deformed crystals where the dislocations act to divide the crystal into a mosaic structure of independently diffracting cells, the kinematical theory may be employed satisfactorily to obtain information on the crystal structure. However, for large single crystals which are also highly perfect, the amplitude of a diffracted wave becomes comparable with that of the incident beam. Interchange of energy

occurs between the beams as they pass through the crystal and a kinematical theory containing an extinction correction cannot be applied. It is necessary to develop a DYNAMICAL theory of diffraction to account for the processes occurring.

The problem can be treated in a variety of ways, and the theory of Darwin, in which the scattered amplitude due to an elementary layer of material is used to obtain a set of differential equations, was originally applied to the two-beam theory of electron diffraction (see Whelan, 1970). However, a more satisfactory approach is that of von Laue (1952) and this is followed here. The dynamical theory in the X-ray case has been excellently reviewed by Batterman and Cole (1964) and Authier (1970) and the reader is strongly recommended to read these articles. More general treatments are to be found in the books by James (1948), Zacharaisen (1945) and von Laue (1960). The article by Hart (1971) on Bragg reflection X-ray optics, referred to again in Chapter 2, also contains a concise summary of the elements of the theory.

1.1. FUNDAMENTAL EQUATIONS OF THE DYNAMICAL THEORY IN A PERFECT CRYSTAL

The problem can be stated with deceptive simplicity. We require a solution of Maxwell's equations in a periodic medium matched to solutions which are plane waves outside the crystal.

The solutions obtained must reflect the periodicity of the crystal lattice, and such functions are known as Bloch functions. The Bloch waves can be constructed from a superposition of plane waves, but it has been verified experimentally that the Bloch waves do have physical significance and are not merely convenient mathematical constructions.

According to the kinematical theory of X-ray diffraction, each diffracted wave is associated with a vector in reciprocal space corresponding to a reciprocal lattice point $\underline{g}$ and also has a wavevector inside the crystal $\underline{K}_g$. The diffracted beam wavevector is related to the wavevector of the incident wave in the crystal by the Laue equation,

$$\underline{K}_g = \underline{K}_o + \underline{g}. \tag{1.2}$$

In the dynamical case, which must yield the same results as the kinematical theory in the limit of thin crystals, we may expect solutions to consist of linear combinations of such waves. Accordingly, we look for solutions of Maxwell's equations for the electric displacement $\underline{D}$ of the form

$$\underline{D} = \sum_g \underline{D}_g \exp(-2\pi i \underline{K}_g . \underline{r}) \exp(i\omega t). \tag{1.3}$$

Assuming that the electrical conductivity is zero and the magnetic permeability is unity, Maxwell's equations reduce to

$$\text{curl curl } \underline{D} = -\{(1 + \chi)/c^2\}(\partial^2 \underline{D}/\partial t^2) . \tag{1.4}$$

In a periodic medium, the susceptibility χ is periodic and can be expanded as a Fourier series over the reciprocal lattice as

$$\chi = \sum_h \chi_h \exp(-2\pi i \underline{h} . \underline{r}). \tag{1.5}$$

χ_h is related to the structure factor F_h by a proportionality constant

$$\chi_h = -r_e\lambda^2 F_h/\pi V_c, \tag{1.6}$$

where r_e is the classical electron radius and V_c is the volume of the unit cell. The structure factor is, of course, related to the atomic scattering factors by

$$F_h = \sum_{\substack{\text{unit}\\ \text{cell}}} f_i \exp(2\pi i \underline{h}.\underline{r}_i), \tag{1.7}$$

where $\underline{r}_i$ is the position vector in real space of the i th atom with respect to the origin.

As χ is very small in the X-ray region, typically of the order of 10^{-5}, we can therefore write (1.4) as

$$\text{curl curl } (1 - \chi)\underline{D} = -(1/c^2)\partial^2\underline{D}/\partial t^2 \tag{1.8}$$

and substitution of (1.3) and (1.5) into (1.8) leads, after some manipulation, to

$$\sum_h \{\chi_{g-h}(\underline{K}_g.\underline{D}_h)\underline{K}_g - \chi_{g-h}(\underline{K}_g.\underline{K}_g)\underline{D}_h\} = \{k^2 - (\underline{K}_g.\underline{K}_g)\}\underline{D}_g, \tag{1.9}$$

where $k = \omega/c$ is the vacuum wavevector.

These equations are the fundamental equations of the dynamical theory and are a vector form of the equivalent equations which may be obtained in the electron case by solving Schrodinger's equation in a periodic medium. Unlike the electron case, it is fortunate in X-ray diffraction that only very rarely does more than one reciprocal lattice point provide a diffracted wave of appreciable amplitude. This arises from the much larger radius of curvature of the Ewald sphere in the electron case compared with X-ray diffraction. Thus, we need only consider two waves to have appreciable amplitude in the crystal - that associated with the incident wave and that associated with the diffracted wave from a reciprocal lattice vector $\underline{g}$. Equations (1.9) then reduce to

$$\chi_g(\underline{K}_g.\underline{D}_o)\underline{K}_g - \chi_g(\underline{K}_g.\underline{K}_g)\underline{D}_o + \chi_o(\underline{K}_g.\underline{D}_g)\underline{K}_g - \chi_o(\underline{K}_g.\underline{K}_g)\underline{D}_g = (k^2 - \underline{K}_g.\underline{K}_g)\underline{D}_g \tag{1.10a}$$

$$\chi_{\bar{g}}(\underline{K}_o.\underline{D}_g)\underline{K}_o - \chi_{\bar{g}}(\underline{K}_o.\underline{K}_o)\underline{D}_g + \chi_o(\underline{K}_o.\underline{D}_o)\underline{K}_o - \chi_o(\underline{K}_o.\underline{K}_o)\underline{D}_o = (k^2 - \underline{K}_o.\underline{K}_o)\underline{D}_o. \tag{1.10b}$$

Taking the scalar product of (1.10a) with $\underline{D}_g$ and (1.10b) with $\underline{D}_o$ and remembering that waves of electric displacement are always transverse (i.e. $\underline{K}_o.\underline{D}_o = \underline{K}_g.\underline{D}_g = 0$), we obtain

$$\left.\begin{aligned} k^2C\chi_{\bar{g}}D_g + \{k^2(1+\chi_o) - \underline{K}_o.\underline{K}_o\}D_o = 0, \\ \{k^2(1+\chi_o) - \underline{K}_g.\underline{K}_g\}D_g + k^2C\chi_g D_o = 0, \end{aligned}\right\} \tag{1.11}$$

where $C = \underline{D}_o.\underline{D}_g = 1$ for σ polarization
$= \cos 2\theta_B$ for π polarization.

For a non-trivial solution

$$\begin{vmatrix} k^2C\chi_{\bar{g}} & k^2(1+\chi_o) - \underline{K}_o.\underline{K}_o \\ k^2(1+\chi_o) - \underline{K}_g.\underline{K}_g & k^2C\chi_g \end{vmatrix} = 0. \tag{1.12}$$

Writing

$$\begin{aligned} \alpha_o &= \tfrac{1}{2}k\{\underline{K}_o.\underline{K}_o - k^2(1+\chi_o)\}, \\ \alpha_g &= \tfrac{1}{2}k\{\underline{K}_g.\underline{K}_g - k^2(1+\chi_o)\}, \end{aligned} \tag{1.13}$$

We arrive at

$$\alpha_o\alpha_g = \tfrac{1}{4}k^2C^2\chi_g\chi_{\bar{g}}. \tag{1.14}$$

1.2. THE DISPERSION SURFACE

We are now in a position to introduce one of the most important and useful concepts relating to dynamical diffraction theory - the dispersion surface. Equation (1.14) is the fundamental relation linking $\underline{K}_o$ and $\underline{K}_g$ in the crystal, and we can represent it geometrically in the following way. About the origin O and the reciprocal lattice point G (where $\vec{OG} = \underline{g}$) draw spheres of radius k. A section through these spheres is shown in Fig. 1.1. Only close to the intersection, the Laue point, will strong diffraction occur as only there is the Laue equation (1.2) satisfied. Now it is easy to see from (1.11) that if no diffracted wave exists (i.e. $\underline{D}_g = 0$), then

$$|\underline{K}_o| \simeq k(1 + \chi_o/2). \tag{1.15}$$

That implies that the wavevector of the wave in the crystal is given by the wavevector in vacuo multiplied by the refractive index. As χ_o is small, $|\underline{K}_o| \simeq k$. A second pair of spheres are drawn about O and G with radius $k(1 + \chi_o/2)$. Far from the Laue point, the tail of the wavevector in the crystal $\underline{K}_o$ will fall on the sphere about O. However, when strong diffraction occurs (1.14) defines the relation between $\underline{K}_o$ and $\underline{K}_g$ and thus the tail cannot lie on the spheres. Figure 1.2 shows the region close to

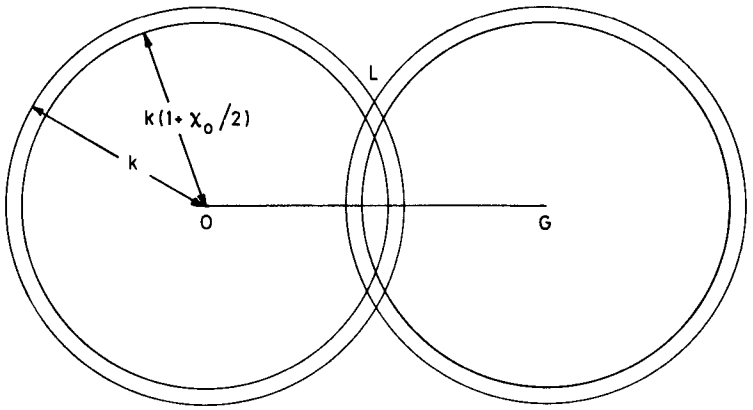

Fig. 1.1. Spheres in reciprocal space about the lattice points O and G showing the position of the Laue point L.

the Laue point at a very much greater magnification.

The arcs AB and A´B´ correspond to the spheres of radius k and the arcs CD and C´D´ to those of radius $k(1 + \chi_o/2)$. The tails of the wavevectors $\underline{K}_o$ and $\underline{K}_g$ lie on the solid curves. We note that α_o and α_g correspond to the perpendicular distances from the point P to the spheres CD and C´D´. As the region is very small compared to the radius of the spheres, the spheres may be approximated as planes. Then the equation of the dispersion surface (1.4) becomes a hyperboloid of revolution with axis OG. Our section of the dispersion surface is thus a hyperbola asymptotic to CD and C´D´. There are four branches - two for each polarization state, the upper ones being denoted branch 1 and the lower ones branch 2. For small Bragg angles the dispersion surfaces of the σ and π polarizations are very close together, but at higher Bragg angles the effects of polarization become extremely important.

Any wave propagating in the crystal must have wavevectors $\underline{K}_o$ and $\underline{K}_g$ lying on the dispersion surface, and returning to (1.3) we see that the wave has amplitude

$$\underline{D} = \exp(i\omega t)\{\underline{D}_o \exp(-2\pi i \underline{K}_o \cdot \underline{r}) + \underline{D}_g \exp(-2\pi i \underline{K}_g \cdot \underline{r})\}, \qquad (1.16)$$

where the amplitudes $\underline{D}_o$ and $\underline{D}_g$ are determined from (1.11) and (1.14). The amplitude ratio

$$R = D_g/D_o = 2\alpha_o/Ck\chi_{\bar{g}} = Ck\chi_g/2\alpha_g. \qquad (1.17)$$

Thus not only can we determine the wavevector from the position of the tie points P on the dispersion surface but also the amplitude. The importance of the construction becomes apparent.